International Journal of Antimicrobial Agents 53 (2019) 508–514

Contents lists available at ScienceDirect

International Journal of Antimicrobial Agents

journal homepage: www.elsevier.com/locate/ijantimicag

In silico studies and evaluation of antiparasitic role of a novel pyruvate phosphate dikinase inhibitor in *Leishmania donovani* infected macrophages

Mohammad Kashif[a], Sumit Kumar Hira[b], Anurag Upadhyaya[c], Uttam Gupta[a], Ranjeet Singh[a], Ankush Paladhi[b], Faez Iqbal Khan[d], Abdur Rub[e], Partha Pratim Manna[a,*]

[a] *Immunobiology Laboratory, Department of Zoology, Institute of Science, Banaras Hindu University, Varanasi, 221005, India*
[b] *Department of Zoology, The University of Burdwan, Purba Bardhhaman, 713104, India*
[c] *Department of Physics, Institute of Science, Banaras Hindu University, Varanasi, 221005, India*
[d] *Computational Mechanistic Chemistry and Drug Discovery, Department of Chemistry, Rhodes University, Grahamstown 6140, South Africa*
[e] *Infection and Immunity Lab, Department of Biotechnology, Jamia Millia Islamia (A Central University), New Delhi, 110025, India*

ARTICLE INFO

Article history:
Received 5 August 2018
Accepted 22 December 2018

Keywords:
In silico
Drug design
Leishmania
Pyruvate phosphate dikinase
Z220582104
Miltefosine

ABSTRACT

The present work deals with the identification and characterization of a novel inhibitor Z220582104, specific to pyruvate phosphate dikinase, for leishmanicidal activities against free promastigotes and intracellular amastigotes. We have used structure-based drug designing approaches and performed homology modelling, virtual screening and molecular dynamics studies. Primary mouse macrophages and macrophage cell line J774A1 were infected with promastigotes of *Leishmania donovani*. Both promastigotes and infected macrophages were subjected to treatment with the varying concentrations of Z220582104 or miltefosine for assessment of leishmanicidal activity. The novel inhibitor Z220582104 demonstrated growth inhibitory potential and reduced the viability of the free promastigotes in a concentration- and time-dependent manner. Z220582104 was also effective against the intracellular form of the parasites and reduced the number of amastigotes in macrophages and also lowered the parasite index, compared with the untreated infected macrophages. Although less effective compared with the miltefosine, Z220582104 is well tolerated by the dividing cells and normal human lymphocytes and monocytes with no adverse effects on the growth kinetics or viability. Our in silico and in vitro studies suggested that *Leishmania donovani* pyruvate phosphate dikinase could be a potential new drug target.

1. Introduction

In humans, *Leishmania* harvests the cholesterol of the cell membrane from macrophages to switch the signalling towards its survival [1,2]. Although chemotherapy is the only available choice of treatment, drug resistance and side effects of the known anti-leishmanial drugs hinder progress in developing an effective therapeutic regimen. Miltefosine, pentavalent antimonials, and other FDA-approved drugs demonstrated treatment failure and resistance [3,4]. Hence, identification of new drug or alternative methods for disease control are needed. Currently, structure-based drug designing (SBDD) strategies are used for the search of new drugs. Virtual screening of new and potentially effective inhibitors against the essential molecules such as enzymes of the parasites and molecular dynamics simulation studies could offer new strategies for treatment of visceral leishmaniasis [5]. SBDD methods could offer cost-effective mechanisms to identify new drugs more comprehensively. The information about the gluconeogenesis in *Leishmania* is insufficient [6]. The enzyme pyruvate phosphate dikinase (PPDK) is one of the key players for the entry of alanine in intracellular amastigotes. It is also reported that mammalian glucogenic precursor L-lactate is also used by amastigotes during the synthesis of its storage carbohydrate mannogen in adverse conditions. This process is mostly facilitated by PPDK [6]. PPDK performs the reversible conversion of PPi, AMP and phosphoenolpyruvate (PEP) into Pi, ATP and pyruvate, respectively [7]. The glycolytic pathway in mammals, including humans, contains pyruvate kinase (PK) instead of PPDK for glucose synthesis. Therefore, the absence of PPDK in mammals and its essential role in parasites makes this enzyme an attractive target for designing anti-leishmanial drugs [8]. We targeted *Leishmania donovani* pyruvate phosphate dikinase (*Ld*PPDK) in search of a new drug which could be of low cost, have less chance of drug resistance and provide better chemotherapeutic

* Corresponding author.
E-mail address: pp_manna@yahoo.com (P.P. Manna).

https://doi.org/10.1016/j.ijantimicag.2018.12.011

results. We have determined the dynamics of anti-leishmanial activity of Z220582104 and compared it with miltefosine against free promastigotes and intracellular amastigotes. Our results suggested that Z220582104 has significant leishmanicidal effects against promastigotes as well as amastigotes.

2. Material and methods

2.1. Structure Prediction and Evaluation

*Ld*PPDK enzyme sequence was retrieved from uniprot (id; E9BAT8). BLASTp server was used for the template identification. Modeller 9.13 was used for homology modelling [9]. Structure Visualization was performed via PyMol [10]. We used multiple sequence alignment (MSA) to find the conserved active site residues [11]. PDBsum server generated the topology of protein.

2.2. Virtual screening

Idock, a multithreaded virtual screening tool for flexible docking, was implemented for virtual screening (http://istar.cse.cuhk.edu.hk/idock/). The tool collected the list of compounds from the ZINC database by applying filters. Nine molecular filters were applied to get the best ligands against the target *Ld*PPDK (Supplementary Table S1).

2.3. Molecular Dynamics Simulation

Molecular dynamics (MD) is a widely used computational method used to simulate biological systems. GROMACS 4.5.5 was used for this purpose [12]. The protein and ligands topology files were created using GROMOS 96 force field and PRODRG2 server [13]. Na^+/Cl^- ions satisfied the electroneutrality conditions [14]. The rest of the parameters were set as described previously [5]. Finally, a 60-ns simulation was performed for all the four complexes and apoprotein. Structural properties were calculated from the trajectory files with the built-in functions such as *g_rmsd, g_rms, g_gyrate, g_dist* and *g_hbond* utilities. GRACE program was implemented for plot generation and outcome extrapolation.

2.4. Parasites, cell lines, reagents and anti-leishmanial drug

L. donovani strain AG83 (MHOM/IN/1983/AG83) was isolated from an Indian kala azar patient [15]. Details of the parasite, cell lines and the culture procedure are given in the Supplementary Material and Methods. Z220582104 (ZINC ID 'ZINC09457211') was obtained from ENAMINE (Cincinnati, OH, USA) and miltefosine was purchased from Sigma, USA.

2.5. Viability and growth Inhibition study

Viability and growth kinetics of promastigotes or tumour cells (JE6.1 and J774A1) were performed in the presence of varying concentrations of Z220582104 or miltefosine. Details are given in the Supplementary Materials and Methods.

2.6. In vitro infection of macrophages and treatment with Z220582104 or miltefosine

Mouse splenic macrophages or J774A1 (5×10^4) cells were cultured on sterile coverslips in culture medium for 3–4 days [15]. Infection in macrophages and leishmanicidal effects of Z220582104 or miltefosine in infected macrophages were described in the Supplementary Materials and Methods [15].

2.7. Statistical analysis

Data are presented as mean ± standard deviation (SD) for multiple experiments (n=3–4). Evaluation of statistical significance was performed by unpaired t test and one- or two-way analysis of variance (ANOVA) and multiple group comparison tests, using PRISM software (Graph Pad). Statistical significance was analysed by log-rank (Mantel Cox) test. $P<0.05$ was considered as statistically significant. $^*P<0.05$, $^{**}P<0.01$, and $^{***}P<0.001$.

3. Results and Discussion

3.1. Ld*PPDK Structure*

The *Ld*PPDK enzyme consists of 914 amino acids. *Trypanosoma brucei* pyruvate phosphate dikinase, *Tb*PPDK (PDB id: 2 × 0S) was selected as a template, having 76% sequence similarity with *Ld*PPDK and was used to construct the model *Ld*PPDK enzyme via Modeller 9.13 (Fig. 1A). The root mean square deviation (RMSD) between the target and template was 0.847 Å (Fig. 1B). The *Ld*PPDK structural topology showed 43 helices, 31 strands and 7 β-sheets (Fig. 1C,D). The model showed 91.8% residues in the most favoured regions, 7.5% in additionally allowed regions and 0.6% in the disallowed regions of the Ramachandran plot, generated by PROCHECK [16] (Supplementary Fig. S1A). The ProSA web-server-based Z-score values of *Ld*PPDK and *Tb*PPDK were -13.86 and -14.32 suggesting reliability of the model (Supplementary Fig. S1B). It also generated the knowledge-based energy profile of the *Ld*PPDK protein (Supplementary Fig. S1C). The catalytic site of the template *Tb*PPDK has Lys-27, Arg-96, Asp-348, Glu-350, and Arg-364 as critical residues (Supplementary Fig. S2A) [17]. MSA data (Supplementary Fig. S2B) showed that the conserved active site residues of *Ld*PPDK are Lys-28, Arg-97, Asp-349, Glu-351 and Arg-365 (Fig. 1A). The pocket coordinates of the enzyme was generated by the Ligsite-csc program [18].

3.2. In silico virtual screening

The idock tool showed the binding energy ranging from -3.68 kcal/mol to -9.95 kcal/mol of screened compounds. The top 10 ligands were selected for the study (Supplementary Table S2). These top 10 compounds were also screened through the iGEMDOCK tool [19] in order to ensure their interactions with *Ld*PPDK (Supplementary Table S2). The top four molecules with ZINC ids, ZINC08297842, ZINC09457211, ZINC36660108 and ZINC40182556 showed binding affinity of -9.95 kcal/mol, -9.83 kcal/mol, -9.63 kcal/mol and -9.61 kcal/mol, respectively. The docked complexes and interaction plots are shown in Supplementary Fig. S3.

3.3. Molecular dynamics simulations

MD simulations of the top four docked complexes were performed, and the generated trajectories were used for the analysis (Fig. 2). The RMSD values of all of the systems were increased in the initial phases during the simulation. The backbone of first complex (*Ld*PPDK-ZINC08297842) showed the higher deflections between 0.51 and 0.62 nm at 5–9 ns and 0.71 nm at 11 ns (green line, Fig. 2). Later, it decreased and converged to 0.66 nm at 60 ns. The *Ld*PPDK-ZINC09457211 complex demonstrated the best-equilibrated trajectories among all the values. It attained the RMSD value of 0.5 nm at 4 ns followed by a drop and later reached 0.64 nm at around 11.0 ns. Finally, the plateau converged at 0.46 nm (blue line, Fig. 2). Similarly, *Ld*PPDK-ZINC36660108 (yellow line, Fig. 2) made higher deflection of 0.62 nm at 19 ns, 0.80–0.91 nm at 28 ns and converged to 0.89 nm at 60 ns. The fourth complex, *Ld*PPDK-ZINC40182556 (purple line, Fig. 2) converged at 0.76

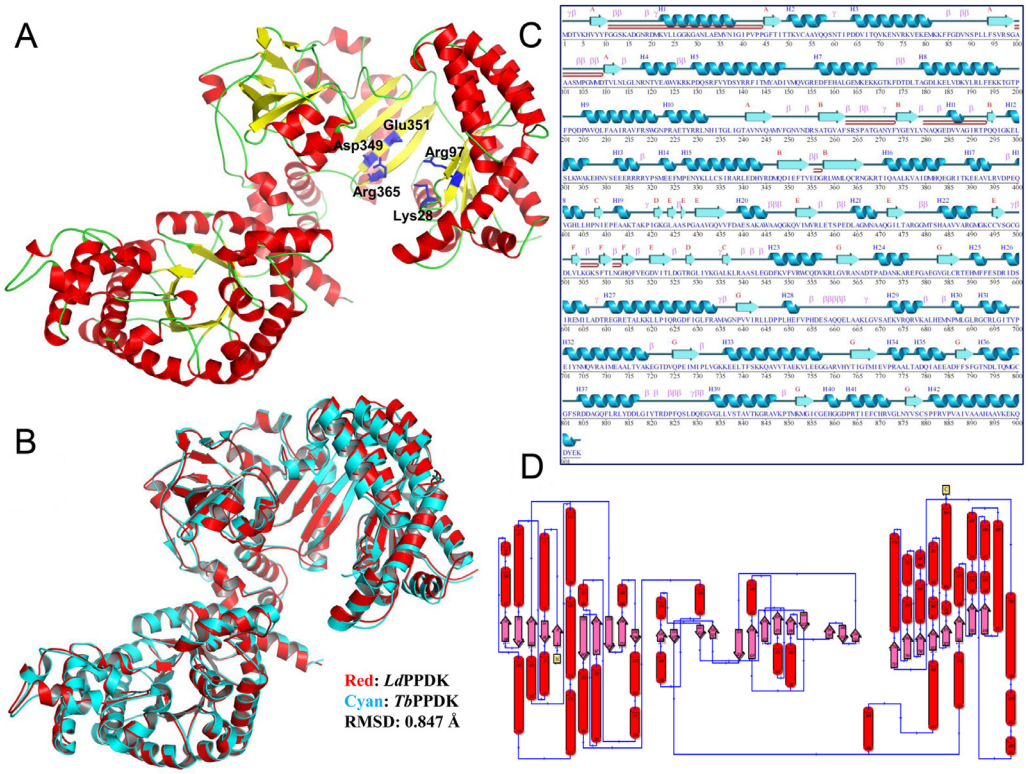

Fig. 1. (A) Cartoon model of LdPPDK enzyme with the predicted active site residues (shown in stick model). (B) Superimposed structure of the target and template enzymes. (C) Secondary structure elements and (D) topology map of LdPPDK enzyme, indicating a conserved α and β framework.

nm finally. The apoprotein backbone showed destabilised trajectories throughout the simulation (black line, Fig. 2) and gets simulated at 0.49 nm. This suggested that compound ZINC09457211 has the lowest RMSD value compared with the other systems and may have the maximum potential to inhibit the *Ld*PPDK activity (Fig. 2A). The backbone root mean square fluctuation (RMSF) values of all the systems demonstrated the movement of each residue. The higher the value of RMSF, the greater will be the flexibility and unstable binding. The active site positions K28, R97, D349 and E351 in *Ld*PPDK-ZINC09457211 complex (blue line, Fig. 2) attained 0.17 nm, 0.11 nm, 0.07 nm and 0.07 nm RMSF values, respectively. These values were lower than the apoprotein RMSF value which suggests that it was the most stable complex (Fig. 2B). The radius of gyration (Rg) analyses the stability of a protein by exploring the tertiary structure volume. A higher value of Rg suggests that the apoprotein has loose packing. The average Rg values for the *Ld*PPDK enzyme, *Ld*PPDK-ZINC08297842, *Ld*PPDK-ZINC09457211, *Ld*PPDK-ZINC36660108 and *Ld*PPDK-ZINC40182556 complexes were 3.51 nm, 3.22 nm, 3.10 nm, 3.27 nm and 3.16 nm, respectively. This plot suggested that *Ld*PPDK attained tight packing after ZINC09457211 binding (Fig. 2C). The average distance between the *Ld*PPDK protein and the compounds were plotted against time. The *Ld*PPDK-ZINC09457211 complex showed distance value of 2.10 nm which was proximal, compared with the rest of the three complexes formed by the other three compounds. The compounds ZINC08297842, ZINC36660108 and ZINC40182556 showed 2.34-, 2.24- and 2.21-nm distances, respectively. The compound ZINC09457211 showed significantly less distance compared with the other three compounds (Fig. 2D). The hydrogen bond analysis during the simulation suggested that the compounds bind with *Ld*PPDK with two to five hydrogen bonds (Supplementary Fig. S4). We used miltefosine, a well-known anti-leishmanial agent as a control drug. The binding affinity of miltefosine was -4.8 kcal/mol and was unable to form any interaction with the conserved active site residues (Supplementary Fig. S5A). The RMSD value of *Ld*PPDK-miltefosine complex attained higher values compared with apoprotein and *Ld*PPDK-ZINC09457211 complex values and converged at 0.69 nm. The RMSF deflection also presented higher flexibility of the backbone made by the *Ld*PPDK-miltefosine complex (Supplementary Fig. S5B).

3.4. Parasite growth Inhibitory effect of Z220582104

Following treatment with Z220582104 for 24 h, the viability of promastigotes was significantly reduced in a concentration-dependent manner (Supplementary Fig. S6). Direct effect of various concentrations of Z220582104 or miltefosine on the growth inhibition of *L. donovani* promastigotes was studied following co-culture of the parasites with the drugs for 8 days at 22°C in M-199 medium (Fig. 3). Compared with the Z220582104, miltefosine has significantly higher growth inhibitory effect against the parasite. Z220582104 at a concentration of 100 µM reduced the growth of the promastigotes by 60% compared to 100% inhibition in the presence of miltefosine. At lower concentrations, Z220582104 became less effective while miltefosine remained significantly leishmanicidal at the concentration of 12.5 µM. Z220582104 was found to be ineffective at lower concentrations (12.5 µM and 6.25 µM) while miltefosine was significantly growth inhibitory to *L. donovani* promastigotes (P <0.01, P <0.001). Z220582104 at 100 µM concentration, inhibited the growth of *L. donovani* promastigotes by 64.45% on day 2, 79.1% on day 4 and 60.8% on day 6 (P<0.0001 for each comparison) (Fig. 3). Lower concentrations (50 and 25 µM) of Z220582104 were also growth inhibitory to *L. donovani* promastigotes although the effect was markedly lower compared to higher concentration. Higher concentrations (>100 µM) of Z220582104 (200, 300 and 400 µM) was significantly more leishmanicidal and nearly achieve comparable performances to that of miltefosine (Supplementary Fig. S7). Z220582104, compared with miltefosine,

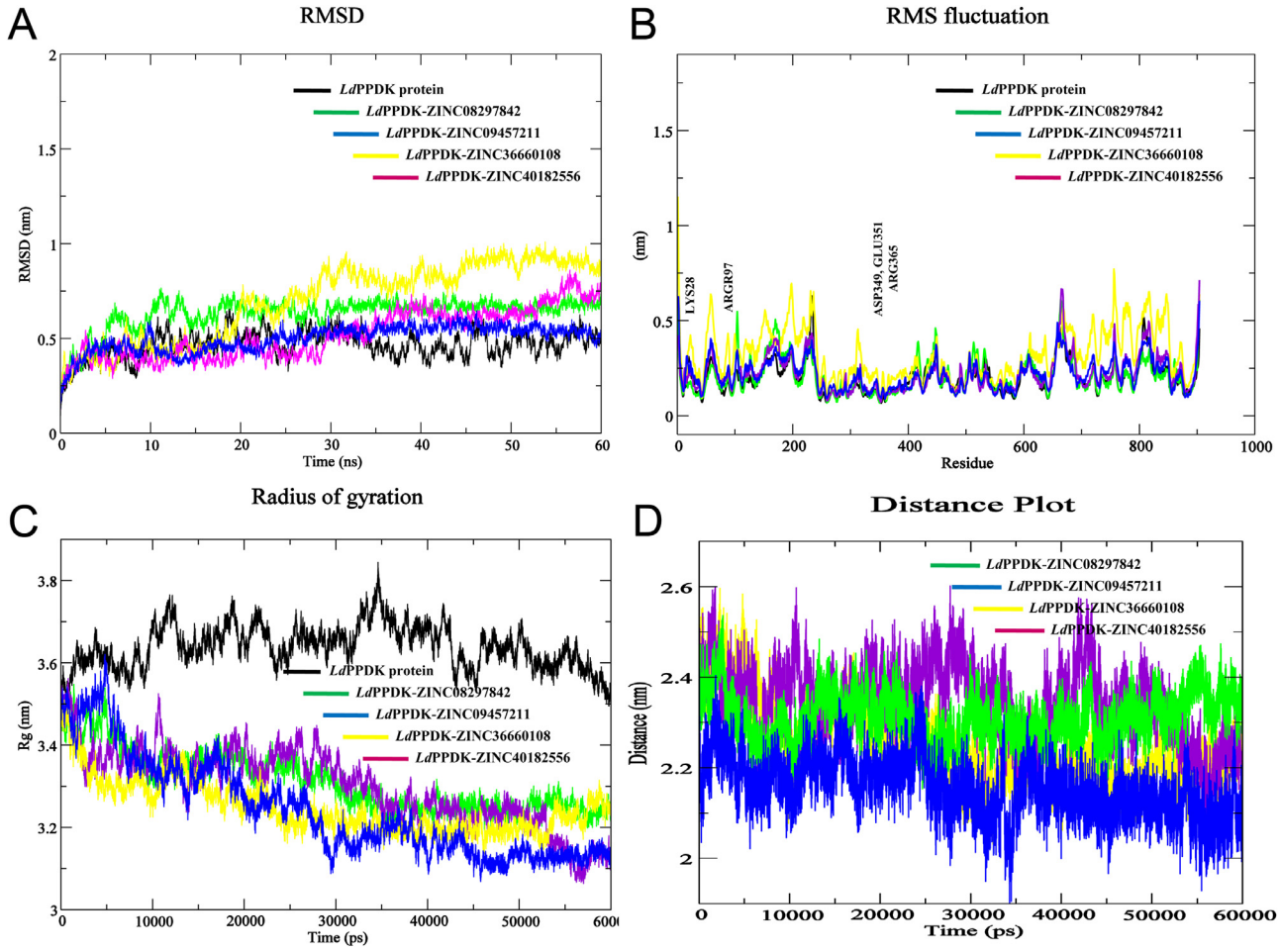

Fig. 2. (A) Root mean square deviation (RMSD) plot as a function of time. Black, green, blue, yellow and purple colours represent the values obtained for free LdPPDK, LdPPDK-ZINC08297842, LdPPDK-ZINC09457211, LdPPDK-ZINC36660108 and LdPPDK-ZINC40182556 complexes, respectively. (B) Root mean square fluctuation (RMSF) of free LdPPDK enzyme (black), LdPPDK-ZINC08297842 (green), LdPPDK-ZINC09457211 (blue), LdPPDK-ZINC36660108 (yellow) and LdPPDK-ZINC40182556 (purple) complexes. (C) Radius of gyration (Rg) values for free LdPPDK enzyme (black), LdPPDK-ZINC08297842 (green), LdPPDK-ZINC09457211 (blue), LdPPDK-ZINC36660108 (yellow) and LdPPDK-ZINC40182556 (purple) complexes. (D) The average distances between the LdPPDK enzyme and the compounds were plotted against time.

was relatively tolerant to dividing cell line JE6.1 as assessed by the viability and growth inhibition kinetics respectively (Supplementary Fig. S8A,B). The viability and growth inhibition experiments on promastigotes suggested that Z220582104 has immediate and long-term anti-promastigote effects comparable to that of miltefosine treatment.

3.5. Anti-leishmanial effect of Z220582104 against infected macrophages

Results from the above experiments suggested that Z220582104 has strong anti-leishmanial effect against free promastigotes. We next wanted to know whether Z220582104 could also restrict the growth and proliferation of intracellular amastigotes in infected BALB/c macrophages. Following treatment with *L. donovani* infected BALB/c splenic macrophages; Z220582104 kills the intracellular amastigotes in a concentration dependent manner. The percent infection in infected macrophages reduced significantly at various concentrations tested (Fig. 4). The percent infected macrophages reduced from 74.48±2.00 in untreated control to 19.26±3.92, 9.82±0.60 and 5.51±1.71 following treatment with 100 µM, 200 µM and 400 µM Z220582104 (Fig. 4A). The amastigotes per 100 macrophages were reduced from 197.50±29.89 in untreated control to 61.12±15.25, 28.95±4.40 and 17.13±3.94 following identical treatment with Z220582104 as mentioned above (Fig. 4A). Miltefosine was found to be significantly more leishmanicidal compared with Z220582104. Percent infected macrophages were reduced to 23.87±2.08, 15.11±2.77 and 13.77±4.13 following treatment with 25µM, 50 µM and 100 µM miltefosine (Fig. 4C). The amastigotes per 100 macrophages were reduced from 197.50±29.89 in untreated control to 67.86±12.65, 37.80±8.25 and 29.12±1.51 respectively (Fig. 4C). On an average, miltefosine is 4 times more effective in leishmanicidal activity against the intracellular amastigotes (Fig. 4B,D). The phagocytic index was reduced from 146.38±18.91 in control group to 12.08±5.11, 2.79±0.28 and 0.92±0.36 following treatment with 100 µM, 200 µM and 400 µM Z220582104 (Fig. 4B). The corresponding results in miltefosine treatment were 16.30±5.08, 5.76±2.23 and 3.97±1.32 following treatment with 25 µM, 50 µM and 100 µM respectively (Fig. 4D). Significant reduction in percent infected macrophages and amastigotes/100 macrophages were observed between the highest and lowest concentrations of miltefosine tested ($P<0.05$, <0.01 and <0.001). Z220582104 requires four-times more drug in order to produce equivalent effects compared with miltefosine. However, Z220582104 has one brighter side in contrast to miltefosine which is toxic to the cells beyond 100 µM, causing extensive cell death and cell lysis. We tested both Z220582104 and miltefosine on the viability and growth inhibition of J774A1 macrophage. Our data suggested that like JE6.1, J774A1 cells also retained the viability in the presence of Z220582104.

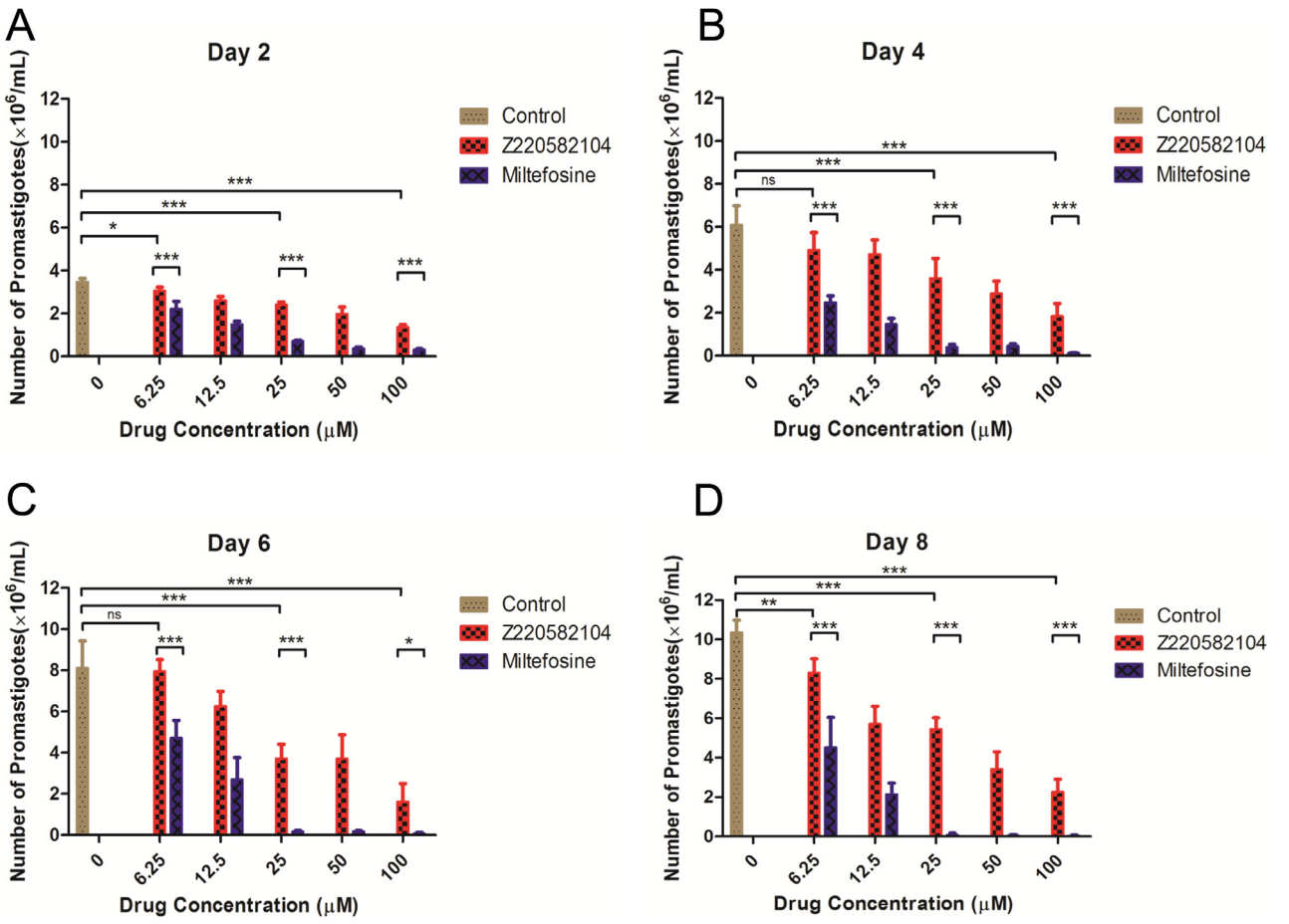

Fig. 3. Dose-dependent growth inhibitory effects of Z220582104 and miltefosine on promastigotes of *Leishmania donovani* for 2, 4, 6 and 8 days. Number of promastigotes was counted following treatment with each concentration of above formulations for the indicated days. $n = 3$.

Cell viability was severely compromised in the presence of miltefosine ($P<0.01$, at 50 μM concentration) (Supplementary Fig. S9A).

Proliferation of dividing cells such as E6.1 or J774A1 for extended periods of time was also affected significantly in the presence of miltefosine compared with Z220582104 ($P<0.01$, 400 vs 6.25 μM), as judged by MTT assay (Supplementary Fig. S9B). Z220582104 remain tolerant to mammalian cells despite the presence of very high concentration (400 μM). We extended our study to examine the role of both the drugs against normal human peripheral blood lymphocytes and monocytes. Our data suggested that Z220582104 is safe with respect to lymphocytes viability, which was severely affected in the presence of miltefosine ($P<0.05$) (Supplementary Fig. S10A). Human monocytes were found to be relatively safe in the presence of comparable concentrations of Z220582104 or miltefosine (Supplementary Fig. S10B). Leishmanicidal effects of Z220582104 and miltefosine were also tested against intracellular amastigotes in J774A1 cells. Similar to splenic macrophages, Z220582104 significantly reduced the percent infected macrophages and amastigotes/100 macrophages compared with the untreated control (Supplementary Fig. S11A). Results on phagocytic index suggested that Z220582104 can be an effective alternative in reducing the parasite burden inside the macrophages without affecting the viability of the host cells ($P<0.001$) (Supplementary Fig. S11B). Miltefosine was also effective against the intracellular parasites in J774A1 cells, similar to that of splenic macrophages (Supplementary Fig. S11A,B). The leishmanicidal effects of Z220582104 and miltefosine against amastigotes of splenic BALB/c macrophages were also documented in the photomicrographs presented in Supplementary Fig. S12. The effects of Z220582104 treatment were remarkably competitive when compared with miltefosine.

We took a bioinformatic approach to identifying a novel inhibitor specific to pyruvate phosphate dikinase of *Leishmania* and tested its anti-leishmanial potential against free and intracellular forms of the parasite. The enzyme is present in a variety of organisms such as trypanosomatids, *Entamoeba histolytica, Giardia lamblia,* thermophilic actinobacteria, leaves and roots of C3 plants and in the mesophyll cells of C4 plants [20]. PPDK has also been reported in the *Wolbachia* endosymbiont found in the filarial worm *Brugia malayi* [21]. In the kinetoplastid parasite *Trypanosoma*, PPDK is located in the glycosomes where it performs a role in pyrophosphate recycling [22]. In single-cell protists and anaerobic bacteria, PPDK plays a role in the novel pyrophosphate-dependent glycolytic pathway, which is the key source of chemical energy in the above organisms due to the absence of proteins which supports the Krebs cycle and oxidative phosphorylation [23–25]. In *Entamoeba histolytica*, PPDK has been reported to exert significant control in glycolytic flux [24]. PPDK gene knockdown experiments in *G. lamblia* have shown that the level of ATP was reduced to 3% compared to the normal level [24]. The search for novel inhibitors against PPDK, focusing on ATP binding as well as inhibition of kinase has also been reported [25]. Due to its absence in higher organisms, PPDK holds significant potential as a selective target for the fabrication of new therapeutic agents against infectious diseases including leishmaniasis.

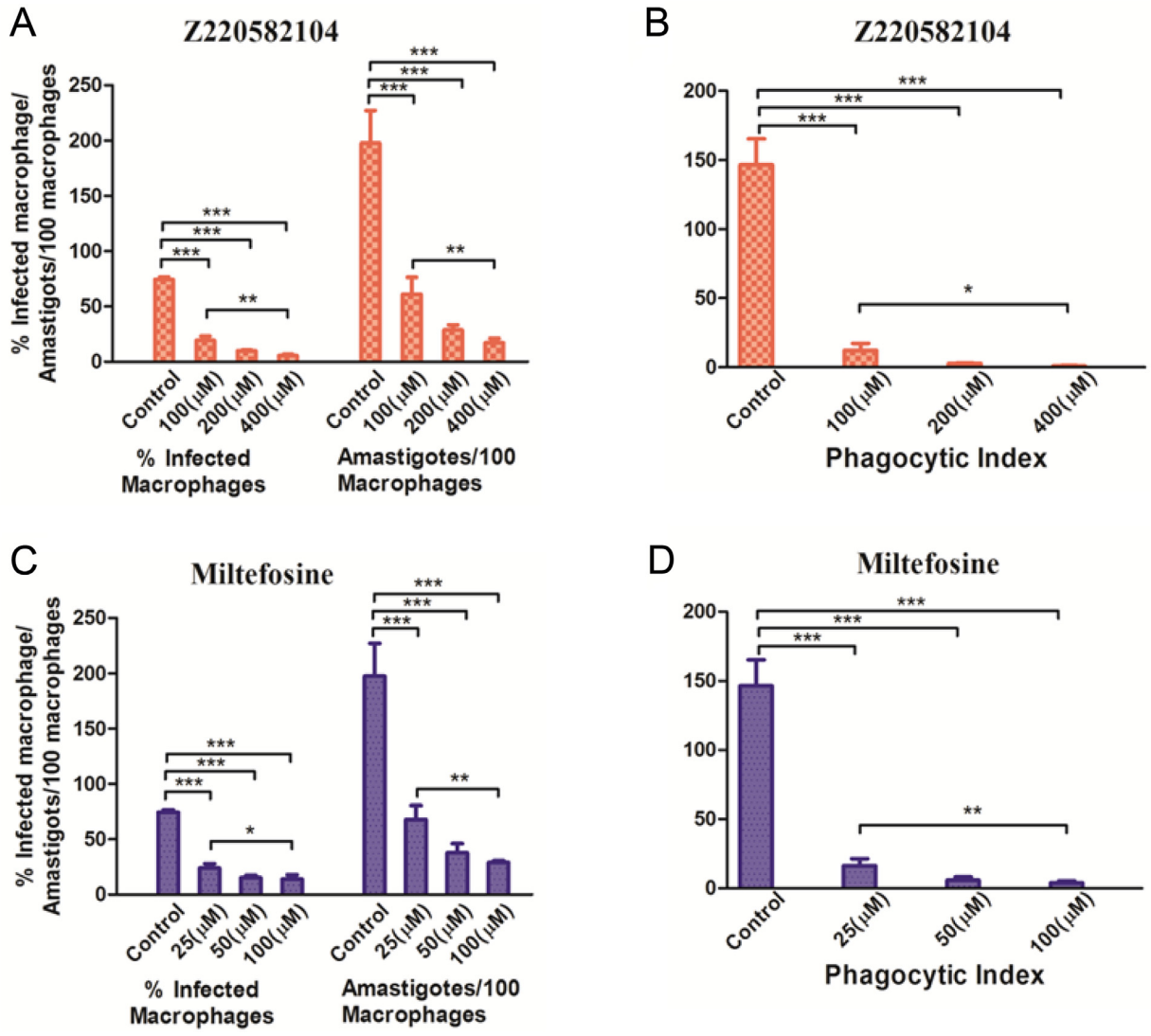

Fig. 4. Antileishmanial activities of Z220582104 and miltefosine against *Leishmania donovani* infected BALB/c splenic macrophages. Anti-leishmanial activity was scored as described in Materials and Methods. (A, C) Percent infected macrophages and amastigotes/100 macrophages following treatment with either Z220582104 or miltefosine; (B, D) the phagocytic index following indicated treatment. Data represents mean ± standard deviation (SD) of quadruplicate determinations. n=4. * <0.05, ** <0.01 and *** <0.001. $n = 4$.

4. Conclusions

Effective vaccines against leishmania infection do not exist, although some groups have developed formulations with acceptable immunogenicity [26].Therapeutic intervention is largely based on chemotherapy including pentavalent antimonials which has long been the cornerstone of the first line of treatment [26,27]. However, treatment with antimonials is associated with several drawbacks including: severe side effects, poor tolerability and critical levels of drug resistance, especially in India [27]. Amphotericin B, pentamidine and miltefosine are the other alternatives which become frontline options for fighting against visceral and cutaneous forms of leishmaniasis, including the antimony-resistant cases [27,28]. The problems become compounded due to the increased rate of resistance and therapeutic failure in critically endemic areas such as India, Africa and South America. Hence, there is an urgent need to explore new drugs that are readily available and affordable for the affected population [29]. Based on the above-mentioned facts and with the objectives to discover active compounds against *Leishmania* that are non-toxic to mammalian cells, we have searched for a novel inhibitor specific to the PPDK of *Leishmania*. The PPDK-specific inhibitor was found to be safe and non-toxic to the mammalian cells even at very high concentrations. At these concentrations, the PPDK inhibitor (Z220582104) is significantly leishmanicidal against the promastigotes and intracellular amastigotes. PPDK has long been considered as a logical target for developing potential herbicides and designing new drugs [30,31]. Our in silico study was aimed at investigating a new inhibitor which is effective against the parasites but tolerant to mammalian cells. The study of PPDK in parasitic organisms is significant because the enzyme is absent in the mammalian host which has different catalytic mechanisms for the glycolytic pathway.

Acknowledgements

Mohammad Kashif is grateful to the Indian Council of Medical Research (ICMR) for Senior Research Fellowship (SRF). The authors also acknowledge Dr. Sanjay Kumar, Department of Physics, BHU for the computational facility.

Funding

This work was partially supported (instrument facility) by a grant from the Department of Biotechnology (DBT), New Delhi, India, No. BT/PR11490/BRB/10/675/2008 (P.P.M.).

Competing Interests

The authors have no conflicts of interest to disclose.

Ethical Approval

Not required.

Supplementary materials

Supplementary material associated with this article can be found, in the online version, at doi:10.1016/j.ijantimicag.2018.12.011.

References

[1] Rub A, Dey R, Jadhav M, Kamat R, Chakkaramakkil S, Majumdar S, et al. Cholesterol depletion associated with Leishmania major infection alters macrophage CD40 signalosome composition and effector function. Nat Immunol 2009;10:273.
[2] Arish M, Husein A, Kashif M, Sandhu P, Hasnain SE, Akhter Y, et al. Orchestration of membrane receptor signaling by membrane lipids. Biochimie 2015;113:111–24.
[3] Jerônimo SMB, Pearson RD. The challenges on developing vaccine against visceral leishmaniasis. Rev Soc Bras Med Trop 2016;49:395–7.
[4] Harms G, Scherbaum H, Reiter-Owona I, Stich A, Richter J. Treatment of imported New World cutaneous leishmaniasis in Germany. Int J Dermatol 2011;50:1336–42.
[5] Kashif M, Tabrez S, Husein A, Arish M, Kalaiarasan P, Manna Partha P, et al. Identification of novel inhibitors against UDP-galactopyranose mutase to combat leishmaniasis. J Cell Biochem 2017;119:2653–65.
[6] Rodriguez-Contreras D, Hamilton N. Gluconeogenesis in Leishmania mexicana: Contribution of glycerol kinase, phosphoenolpyruvate carboxykinase, and pyruvate phosphate dikinase. J Biol Chem 2014;289:32989–3000.
[7] Palayam M, Lakshminarayanan K, Radhakrishnan M, Krishnaswamy G. Preliminary analysis to target pyruvate phosphate dikinase from wolbachia endosymbiont of Brugia malayi for designing anti-filarial agents. Interdiscip Sci 2012;4:74–82.
[8] Stephen P, Vijayan R, Bhat A, Subbarao N, Bamezai RNK. Molecular modeling on pyruvate phosphate dikinase of Entamoeba histolytica and in silico virtual screening for novel inhibitors. J Comput Aided Mol Des 2008;22:647–60.
[9] Šali A, Blundell TL. Comparative Protein modelling by satisfaction of spatial restraints. J Mol Biol 1993;234:779–815.
[10] Lill MA, Danielson ML. Computer-aided drug design platform using PyMOL. J Comput Aided Mol Des 2011;25:13–19.
[11] Thompson JD, Higgins DG, Gibson TJ. CLUSTAL W: improving the sensitivity of progressive multiple sequence alignment through sequence weighting, position-specific gap penalties and weight matrix choice. Nucleic Acids Res 1994;22:4673–80.
[12] Pronk S, Páll S, Schulz R, Larsson P, Bjelkmar P, Apostolov R, et al. GROMACS 4.5: a high-throughput and highly parallel open source molecular simulation toolkit. Bioinformatics 2013;29:845–54.
[13] van Aalten D.M., Bywater R., Findlay J.B., Hendlich M., Hooft R.W., Vriend G. 1996. PRODRG, a Program for Generating Molecular Topologies and Unique Molecular Descriptors from Coordinates of Small Molecules, vol 10.
[14] Baig MH, Sudhakar DR, Kalaiarasan P, Subbarao N, Wadhawa G, Lohani M, et al. Insight into the effect of inhibitor resistant S130G mutant on physico–chemical properties of SHV type beta-lactamase: a molecular dynamics study. PLoS One 2014;9:e112456.
[15] Manna PP, Chakrabarti G, Bandyopadhyay S. Innate immune defense in visceral leishmaniasis: Cytokine mediated protective role by allogeneic effector cell. Vaccine 2010;28:803–10.
[16] Laskowski RA, Rullmann JAC, MacArthur MW, Kaptein R, Thornton JM. AQUA and PROCHECK-NMR: Programs for checking the quality of protein structures solved by NMR. J Biomol NMR 1996;8:477–86.
[17] Cosenza LW, Bringaud F, Baltz T, Vellieux FMD. The 3.0Å resolution crystal structure of glycosomal pyruvate phosphate dikinase from Trypanosoma brucei. J Mol Biol 2002;318:1417–32.
[18] Huang B, Schroeder M. LIGSITE(csc): predicting ligand binding sites using the Connolly surface and degree of conservation. BMC Struct Biol 2006;6:19.
[19] Mohammad K, Partha PM, Yusuf A, Mohammed A, Abdur R. Screening of novel inhibitors against Leishmania donovani calcium ion channel to fight Leishmaniasis. Infect Disord Drug Targets 2017;17:120–9.
[20] Deramchia K, Morand P, Biran M, Millerioux Y, Mazet M, Wargnies M, Franconi J-M, Bringaud F. Contribution of pyruvate phosphate dikinase in the maintenance of the glycosomal ATP/ADP balance in the Trypanosoma brucei procyclic form. J Biol Chem 2014;289:17365–78.
[21] Raverdy S, Foster JM, Roopenian E, Carlow CKS. The Wolbachia endosymbiont of Brugia malayi has an active pyruvate phosphate dikinase. Mol Biochem Parasitol 2008;160:163–6.
[22] Acosta H, Dubourdieu M, Quiñones W, Cáceres A, Bringaud F, Concepción JL. Pyruvate phosphate dikinase and pyrophosphate metabolism in the glycosome of Trypanosoma cruzi epimastigotes. Comp Biochem Physiol Biochem Mol Biol 2004;138:347–56.
[23] J.S. Marshall, A.R. Ashton, Govers F., A.R. Hardham. 2001. Isolation and characterization of four genes encoding pyruvate, phosphate dikinase in the oomycete plant pathogen Phytophthora cinnamomi, vol. 40.
[24] Feng X-M, Cao L-J, Adam RD, Zhang X-C, Lu S-Q. The catalyzing role of PPDK in Giardia lamblia. Biochem Biophys Res Commun 2008;367:394–8.
[25] Minges A, Groth G. Small-molecule inhibition of pyruvate phosphate dikinase targeting the nucleotide binding site. PLoS One 2017;12:e0181139.
[26] Taha M, Ismail NH, Imran S, Anouar EH, Selvaraj M, Jamil W. Synthesis and molecular modelling studies of phenyl linked oxadiazole-phenylhydrazone hybrids as potent antileishmanial agents. Eur J Med Chem 2017;126:1021–33.
[27] Hussain H, Al-Harrasi A, Al-Rawahi A, Green IR, Gibbons S. Fruitful decade for antileishmanial compounds from 2002 to late 2011. Chem Rev 2014;114:10369–428.
[28] Mendoza-Martínez C, Galindo-Sevilla N, Correa-Basurto J, Ugalde-Saldivar VM, Rodríguez-Delgado RG, Hernández-Pineda J, et al. Antileishmanial activity of quinazoline derivatives: Synthesis, docking screens, molecular dynamic simulations and electrochemical studies. Eur J Med Chem 2015;92:314–31.
[29] Tiuman TS, Santos AO, Ueda-Nakamura T, Filho BPD, Nakamura CV. Recent advances in leishmaniasis treatment. Int J Infect Dis 2011;15:e525–32.
[30] Wu C, Dunaway-Mariano D, Mariano PS. Design, synthesis, and evaluation of inhibitors of pyruvate phosphate dikinase. J Org Chem 2013;78:1910–22.
[31] Saavedra E., Pérez-Montfort R. 1996. Energy production in Entamoeba histolytica: New perspectives in rational drug design, vol 27.